DALTON
FULL PAPER

Combined visible spectroscopy–conductance–electrospray mass spectrometry studies of paramagnetic catalysts. Speciation of Jacobsen's manganese salen complex † in the presence of σ-donor ligands, hydroxide sources, and cumyl hydroperoxide ‡

John R. Chipperfield,*[a] John Clayton,[a] Siraj A. Khan[a] and Simon Woodward *[b]

[a] *Department of Chemistry, University of Hull, Kingston-upon-Hull, UK HU6 7RX*
[b] *School of Chemistry, Nottingham University, University Park, Nottingham, UK NG7 2RD*

Received 8th February 2000, Accepted 21st February 2000

Combined multi-technique (visible spectroscopy, conductance, electrospray MS) experiments have been applied to the study of Jacobsen's manganese salen complex, **JCl**. Equilibria between **JCl** and σ-donors L (heterocyclic amines and 4-phenylpyridine *N*-oxide) form labile octahedral salts **[J(L)$_2$]Cl** as the major solution species. Many samples of **JCl** are found occasionally to contain small amounts of an impurity whose kinetic behaviour suggest it is **JOH**. The compound **JOH** may also be generated by Bu_4NOH addition to **JCl**. In the presence of an excess of cumyl hydroperoxide CHP and *N*-methylimidazole, **JOH** is converted into a green intermediate, characterised by mass spectrometry as **[J$_2$(O)]$^+$**. This intermediate undergoes first-order decomposition in the presence of CHP regenerating **JOH**.

Introduction

Some of the most effective asymmetric oxidation catalysts are the remarkable manganese salen-derived complexes, first described by Jacobsen, of which **JCl** is the most successful example (see Scheme 1 for nomenclature).[1] Compound **JCl** catalyses the epoxidation of *cis*-substituted alkenes with very high enantioselectivity using various terminal O-atom sources.

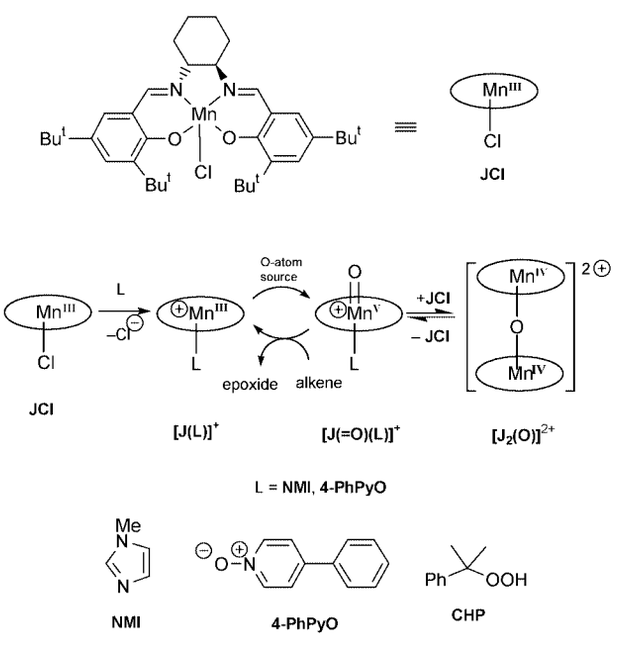

Scheme 1

† [(*R*,*R*)-(−)-*N*,*N*′-Bis(3,5-di-*tert*-butylsalicylidene)-1,2-cyclohexanediaminato]manganese(III) chloride.
‡ Electronic supplementary information (ESI) available: derivations, absorbance and conductance data. See http://www.rsc.org/suppdata/dt/b0/b001059f/

However, while NaOCl,[2] H_2O_2,[3] $NaIO_4$,[4] peracids[5] and PhIO[6] are all effective in these reactions, use of hydroperoxides (for example, cumyl hydroperoxide, $PhCMe_2OOH$, CHP) leads to no epoxidation activity. The general features of the successful epoxidations are in accord with the catalytic cycle (Scheme 1) originally proposed by Kochi and co-workers.[6] Species closely related to the key manganese(V) oxo species have been detected by electrospray mass spectrometry.[7] These manganese(V) oxo species add an additional manganese(III) salen complex resulting in a Mn^{IV}_2 μ-oxo dimer as the catalytic rest state.[6] Both the rate and selectivity of epoxidations catalysed by compound **JCl** are promoted by the addition of σ-donor ligands whose proposed role is to stabilise the manganese(V) oxo species in the catalytic cycle.[8] However, characterisation of the species present in catalytic cycles promoted by **JCl** is complicated by their paramagnetic nature that prevents the use of NMR methods. We proposed using combined visible spectroscopy–conductance–electrospray mass spectrometry techniques as an alternative approach to deriving mechanistic, and rate, information from such paramagnetic catalysts. As a test of the utility of this combined technique approach reactions of **JCl** with σ-donor ligands (such as *N*-methylimidazole, $MeNC_3H_2N$, NMI) and cumyl hydroperoxide have been studied. Specifically we aimed to: (i) quantify σ-ligand binding to **JCl** and (ii) identify the reasons why hydroperoxides are poor terminal oxidants for epoxidations with this class of catalyst.

Results and discussion

Reaction of Jacobsen's catalyst JCl with *N*-methylimidazoles and related σ-donors

As the concentration of NMI is increased (0–125 mM) in a 1.0 mM acetonitrile solution of Jacobsen's catalyst **JCl** a subtle change is evident in the visual spectrum with the observation of a clean isosbestic point at 476 nm (Fig. 1). More concentrated solutions of **JCl** cannot be used due to its high molar absorptivity. The observation of a *single* isosbestic point is most simply explained by clean transformation of **JCl** into a *single* major

DOI: 10.1039/b001059f

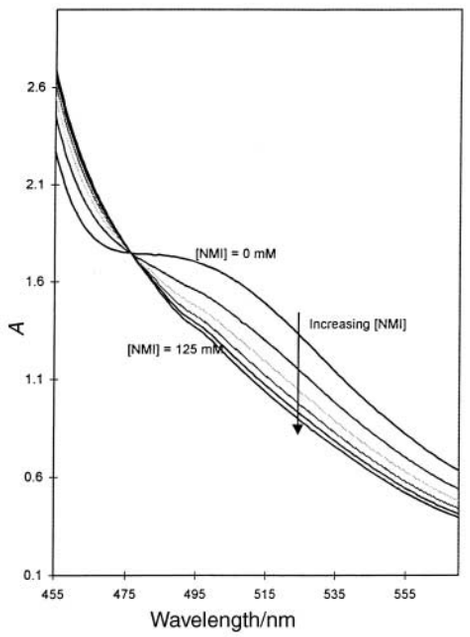

Fig. 1 Visible spectra resulting from successive addition of NMI to **JCl** (1.0 mM) in acetonitrile at 20 °C.

species. Both before and after addition of the NMI the solutions are EPR silent consistent with both species being manganese(III) and showing that reduction to Mn^{II} does *not* occur.[9]

Three models can be proposed that are consistent with these observations: the formation of octahedral **J(L)Cl**, the five-coordinate salt **[J(L)]Cl**, or the octahedral salt **[J(L)$_2$]Cl** (Scheme 2, equilibria 1–3, L = NMI). Conductance data are useful to distinguish between these possibilities. Control runs indicate only a slight increase in the conductance of acetonitrile due to

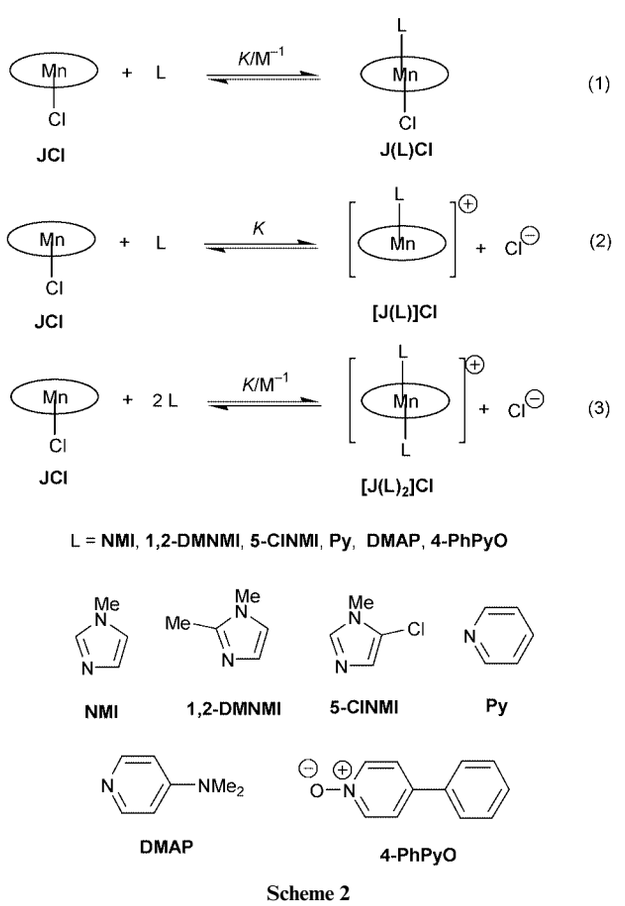

Scheme 2

Table 1 Binding constants (as K) values for the formation of **[J(L)$_2$]Cl** from **JCl**

Donor ligand	Binding constant K (equation 3)/M^{-1}	pK_a(HL)$^+$ (ref.)
NMI	0.36	6.0 (10)
1,2-DMNMI	0.09	7.87 (10)
5-ClNMI	0.007	5.10 (10)
Py	0.03	5.24 (11)
DMAP	0.81	9.55 (12)
4-PhPyO	0.17	0.83 (13)

added NMI in the absence of **JCl**. We attribute this very slight increase to traces of water contamination in the NMI; this was corrected for in the **JCl**/NMI system. At 25 °C the specific conductance (κ) of 1.0 mM solutions of Jacobsen's catalyst **JCl** is 2.91×10^6 S cm^{-1}. This value increases over ten times to 34.5×10^6 S cm^{-1} once a 25 fold excess of NMI is present. At 124 mM NMI and 1.0 mM **JCl** the conductance is 74.3×10^6 S cm^{-1}. This value compares very well with that observed for a 1.0 mM solution of HNMI$^+$Cl$^-$ in dry acetonitrile in the presence of 122 mM NMI (65.4×10^6 S cm^{-1}). Thus, clear ionisation of **JCl** takes place and equilibrium (1) may be rejected on these grounds. Equilibria (2) and (3) were defined and both the absorption and conductance data simulated (see Supplementary data). For a series of additions of aliquots of NMI to a solution of **JCl** the expected absorbances can be calculated from the concentrations of reactants, the equilibrium constant K, and $\varepsilon_{complex}$. The 'best-fit' values for K and $\varepsilon_{complex}$ were calculated by minimising $\Sigma(obs. - calc.)^2$. A similar calculation applies to conductance data. A typical experiment took 1 mM **JCl** in acetonitrile, and portions of NMI were added to increase its concentration in 25 mM steps. Both conductance and absorbance at 550 nm were recorded. For absorbance data $\Sigma(obs. - calc.)^2 = 0.001$ (equilibrium 2) and 4×10^{-5} (equilibrium 3). For conductance data $\Sigma(obs. - calc.)^2 = 10.2$ (equilibrium 2) and 3.3 (equilibrium 3). For both physical properties these data lead to the conclusion that **[J(L)$_2$]Cl** (L = NMI) is the major species in equilibrium with **JCl** with $K = 0.30 \pm 0.02$ (absorbance) and 0.35 ± 0.04 M^{-1} (conductance). This value of K is temperature independent, within the range reported here. Spectrometry and conductivity data at 20 °C give $K = 0.36 \pm 0.14$ M^{-1}. Most results were obtained at this latter temperature. Equilibrium (3) is promoted by the addition of water, and experiments performed under conditions that are not rigorously anhydrous lead to slightly higher K values. Similar experiments were carried out with other heterocyclic donors and with 4-phenylpyridine *N*-oxide. The results of these experiments are summarised in Table 1 (for definitions of the abbreviations and the ligand structures see Scheme 2). Rewardingly both the visual spectroscopy and conductance data give identical values for the equilibrium constants within experimental error.

The behaviour of 1,2-dimethylimidazole 1,2-DMNMI and 5-chloroimidazole 5-ClNMI is similar to that of the parent NMI except that smaller changes in the molar absorbance and conductance are observed. Applying equilibria analogous to (2) gives a lower binding constant for 1,2-DMNMI. The binding of 5-ClNMI was so small that only a lower limiting value for K could be obtained. We ascribe these lower binding constants to steric clashes with the metal complex in the case of 1,2-DMNMI and to inductive weakening of the donor basicity for 5-ClNMI. Similarly pyridine Py is bound about 20 times more weakly than the more electron rich 4-dimethylaminopyridine DMAP. There is some correlation between the size of the binding constants K and the pK_a values of the conjugate acids HL$^+$ of the donor ligands (Table 1). An exception to this is the behaviour of 1,2-DMNMI. The higher pK_a value does not take into account the steric clashes involved in binding the

manganese complex *vs*. a proton. Additionally, 4-phenylpyridine *N*-oxide 4-PhPyO has a relatively high binding constant even though it is more acidic. Given that pK_a is essentially only a measure of σ-donor power this may be indicative of some π donation by 4-PhPyO.

While the data obtained here suggest a significant weighting towards species of type **[J(L)$_2$]Cl** it is important to realise in high spin d^4 Jahn–Teller distorted species that axial co-ordination sites are very labile. Crystallographically characterised manganese(III) salen complexes show Mn^{III}–L_{axial} distances of 2.2–2.3 Å compared to 1.95–2.15 Å for Mn^{III}–N_{imine} and 1.85–1.9 Å for Mn^{III}–$O_{phenolate}$ bonds, reinforcing this idea.[14] When **JCl** (1 mM) is mixed with 125 mM NMI, **[J(NMI)$_2$]Cl** represents some 90% of the solution species present (based on the calculated value of *K*). This picture is consistent with crystallographic data where manganese(III) salen cations generally exist as bis solvates in the solid state.[15,16] After the addition of σ donors to **JCl** it is clear that **[J(L)$_2$]Cl** are present as a major species under the large excess of **L** employed here. However, the five-co-ordinate species **[J(L)]Cl** will be readily formed under conditions favouring ligand dissociation. Interestingly in this respect the visible spectroscopy data from the interaction of 1,2-dimethylimidazole 1,2-DMNMI with **JCl** shows slight evidence of a second isosbestic point at *ca*. 650 nm. Such behaviour would be consistent with a mixed equilibrium leading to small amounts of five-co-ordinate **[J(1,2-DMNMI)]Cl**. The ready accessibility of five-co-ordinate species, *via* ligand dissociation, in these systems is supported by electrospray mass spectrometry (ESMS) studies.

Electrospray mass spectrometry. Positive ion ESMS of a 1 mM MeCN solution of Jacobsen's catalyst **JCl** shows no molecular ion. Conductance studies and literature data[15] confirm that only **JCl** is present in the solution entering the mass spectrometer. A strong peak at *m*/*z* 599 corresponding to **J**$^+$ is seen. Additionally, peaks are observed at *m*/*z* 1233 and 1869 whose isotope patterns confirm them to be **[J$_2$(Cl)]**$^+$ and **[J$_3$(Cl)$_2$]**$^+$ (for nomenclature see Schemes 1, 2). Secondary fragmentation analysis of these ion-trapped species indicates weak chloro bridging ligands. For example, secondary fragmentation of the *m*/*z* 1233 peak leads only to **J**$^+$. As our conductance studies give no evidence for spontaneous ionisation of **JCl** in acetonitrile it is clear that these chloro-bridged oligomers are generated during the electrospray ionisation and are not present in the **JCl** solution. This is supported by the

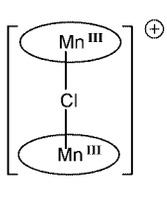

[J$_2$(Cl)]$^+$

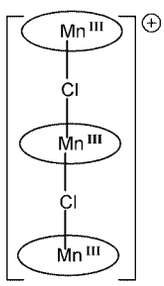

[J$_3$(Cl)$_2$]$^+$

fact that the intensity of the *m*/*z* 1233 and 1869 features is highly dependent on the ESMS conditions (flow rates and capillary temperature).

On addition of NMI to the **JCl** solution the spectrum is largely unchanged but two new major reproducible peaks are observed. These are assigned to **[J(NMI)]**$^+$ (*m*/*z* 681) and **[J(MeCN)]**$^+$ (*m*/*z* 639). No signal for **[J(NMI)$_2$]**$^+$ could be identified. Apparently it does not survive heating in the ES capillary (200 °C) or under the ES ionisation conditions facile NMI dissociation occurs. Related loss of one axial ligand from bis adducts of manganese(III) salen complexes is known.[14]

Reaction of Jacobsen's catalyst JCl with PhCMe$_2$OOH in the presence of NMI and hydroxide sources

Formation of the green intermediate [J$_2$(O)]$^+$**.** Experimentally it is found that when some (but not all) sources of **JCl** are treated with PhCMe$_2$OOH, in the presence of an excess of NMI, a green colour is formed which then fades with time. As the green colour intensifies the solution conductance falls while simultaneously a peak in the mass spectrum at *m*/*z* 1214 grows in intensity. The isotope pattern of this latter peak is consistent with the formulation **[J$_2$(O)]**$^+$. This species, presumably a manganese(III,IV) μ-oxo species (of which examples are known[17]), is the origin of the green colour. Sources of **JCl** which give the most intense green colour are those which have been exposed to sources of hydroxide during their preparation. (Literature preparation of **JCl** often involves deprotonation of the salen ligand by KOH; normally a slight excess of hydroxide is used in these reactions.[18]) This "hydroxide effect" can be confirmed by dosing "inactive" **JCl** sources with NBu$_4$OH. Under these conditions, all samples of **JCl** lead to the green intermediate **[J$_2$(O)]**$^+$ in the presence of CHP and NMI. The starting material in these reactions is effectively [**JCl** + OH$^-$]. This mixture is equivalent to the species "**JOH**" and it is convenient to define it as the starting material for the oxidation. (Analysis of these solutions by simultaneous ESMS/conductance/vis spectroscopy monitoring indicates that although the visible spectrum remains the same if hydroxide is added **JCl** is cleanly consumed. Additionally, a porphyrin analogue of **JOH** has recently been isolated.[19]) The kinetics for the formation of the green intermediate **[J$_2$(O)]**$^+$ was followed using **JCl** synthesized in-house (containing ≈3 mol% **JOH**) or by using samples of **JOH** generated by *in situ* mixing of pure **JCl** and Bu$_4$NOH. As **JCl** scavenges OH$^-$ so effectively care was taken to avoid the adventitious inclusion of hydroxide contaminants in the NMI or solvents employed in these reactions. Owing to these experimental procedures all of the reactions of **JOH**/NMI/CHP in this study take place in the presence of an *excess* of **JCl** and this is always detected in the electrospray mass spectra in the evolving reaction system. Thus, the kinetic data interrogate the nature and reactivity of the **JOH** impurity in samples of **JCl**. Control reactions indicated that **JCl** free of hydroxide impurities does not react with equivalent amounts of CHP in the presence of an excess of NMI.

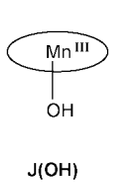

J(OH)

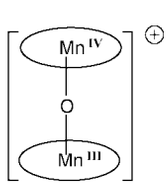

[J$_2$(O)]$^+$

The reaction of 1 mM typical synthetic grade **JCl** (containing ≈0.03 mM **JOH**) with CHP (0.1–5.0 mM) in the presence of an excess of NMI (125 mM) follows a second-order equal concentrations kinetic rate law up to more than 4 half-lives (based on both absorbance and conductance data). The rapid production of a green product is paralleled by a conductance decrease, as expected for an oxidative dimerisation of **JOH** to green **[J$_2$(O)]**$^+$ (the number of charge carriers falls). The same k_2^{obs} is found by analysis of conductance–time and absorbance–time data. For the reaction $X + X \xrightarrow{k_2^{obs}}$ Product, eqn. (4) is the

$$A_t = A_\infty + \frac{A_0 - A_\infty}{1 + [X_o][k_2^{obs}]t} \quad (4)$$

integrated rate equation, where A_t, A_0 and A_∞ are absorbances (or conductances) at time *t*, zero, and infinity; [X$_o$] is the

Table 2 Rate constants (k_2^{obs}) and ΔA values for reaction of **JOH** with CHP in the presence and absence of NMI

[JCl_{tot}]/mM	[OH^-]/mM	[NMI]/mM	[CHP]/mM	ΔA	$k_2^{obs}/M^{-1}\ s^{-1}$ [a]
1.0 [b]	—	—	1.0	0.51	6.58
1.0 [b]	—	125	0.1	0.207	47.0
1.0 [b]	—	125	0.25	0.327	50.6
1.0 [b]	—	125	0.38	0.404	52.3
1.0 [b]	—	125	0.5	0.429	67.5
1.0 [b]	—	125	0.75	0.478	80.5
1.0 [b]	—	125	1.0	0.501	95.2
1.0 [b]	—	125	3	0.569	211
1.0 [b]	—	125	5	0.621	334
1.0 [c]	—	125	1.0	0.303	18.1
1.0 [c]	0.05	125	1.0	0.336	53
1.0 [c]	0.1	125	1.0	0.402	73
1.0 [c]	0.15	125	1.0	0.379	122
1.0 [c]	0.2	125	1.0	0.806	229
1.0 [c]	0.4	125	1.0	0.617	233
1.0 [c]	1.0	125	1.0	0.583	≈1385

[a] From absorbance–time data using eqn. (4) with $[X_0] = [JCl_{tot}]$. [b] Synthetic **JCl** containing 0.03 mM **JOH**. [c] Aldrich reagent grade **JCl** containing 0.01 mM **JOH**.

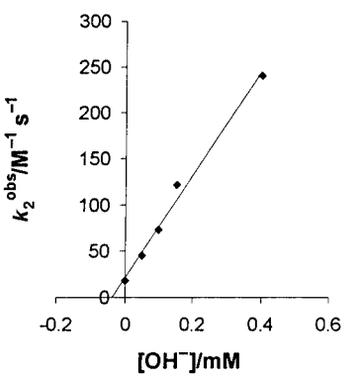

Fig. 2 Variation of k_2^{obs} with concentration of added hydroxide ions for commercial reagent grade **JCl** (Aldrich) reacting with 1.0 mM CHP in the presence of 125 mM NMI in acetonitrile at 20 °C.

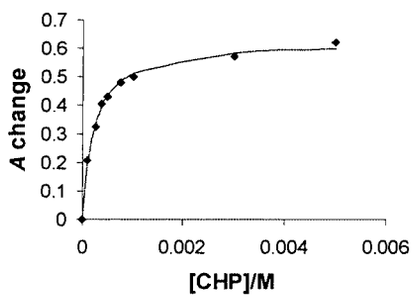

Fig. 3 Absorbance change (ΔA) for reaction of synthetic grade **JCl** (1.0 mM, containing ≈0.03 mM **JOH**) in the presence of 125 mM NMI with varying CHP concentrations in acetonitrile at 20 °C. The line is the best fit of eqn. (10) to the data.

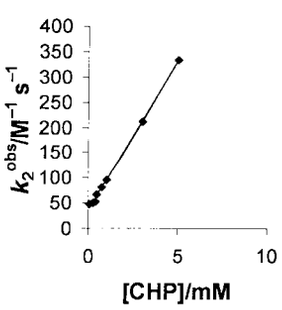

Fig. 4 Variation of k_2^{obs} with CHP concentration for reaction of synthetic grade **JCl** (1.0 mmol, containing ≈0.03 mM **JOH**) in the presence of 125 mM NMI in acetonitrile at 20 °C.

concentration of X at the start. Because **JOH** in all catalytic runs represents a small fixed fraction of the impure Jacobsen's catalyst **JCl** the data are conveniently analysed by letting X be the concentration [JCl_{tot}], eqn. (5) where [JCl_{tot}] is the

$$[JCl_{tot}] = [JCl_{actual}] + [JOH] \quad (5)$$

concentration of the impure Jacobsen's catalyst used in the kinetic run. Experiments involving the generation of **JOH** by addition of Bu_4NOH to pure **JCl**, in the presence of NMI, lead to similar kinetics and the rate constant for the formation of the intermediate, k_2^{obs}, is linearly dependent on the amount of added OH^- (Table 2, Fig. 2). The graph indicates that typical commercial (Aldrich) reagent grade **JCl** catalyst contains 3.8 mol% of **JOH**. Additional support for the involvement of **JOH** comes from the fact that the presence of small amounts of acid (0.2 mM HCl in MeCN/NMI) totally suppresses the formation of the green intermediate $[J_2(O)]^+$. Protonation of the **JOH** impurity generates inactive **JCl** consistent with this picture. If the intermediate is generated in the absence of added NMI its rate of formation is dramatically slowed (Table 2). The role of the NMI may be to co-ordinate free sites in the intermediates leading to $[J_2(O)]^+$.

The second-order equal-concentration kinetic fit for the formation of $[J_2(O)]^+$ from impure Jacobsen's catalyst containing hydroxide impurities **JOH** is essentially perfect over >2000 data points for all runs at different CHP concentrations (0.1 to 5.0 mM). For this simple kinetic regime (eqn. (4)) both the measured change in absorbance (ΔA) and value of the derived rate constant k_2^{obs} should *not* depend on the CHP concentration as this does not appear in eqn. (4). This is *not* the case. Both are CHP concentration dependent: absorbance change (Fig. 3) and observed rate (Fig. 4). The only kinetic models that rationalise these observations involve equilibrium binding of the CHP to the starting material **JOH** or the product $[J_2(O)]^+$. These reaction intermediates cannot be isolated but the proposed structures contain free axial co-ordination sites capable of binding CHP as a σ donor.

The observed rise in absorbance (ΔA) for the formation of $[J_2(O)]^+$ gives a reciprocal fit (eqn. (6)) with $a = 0.62$, $K = 4000$

$$\Delta A = aK[CHP]/(1 + K[CHP]) \quad (6)$$

M^{-1} while k_2^{obs} is linearly dependent on CHP concentration (Fig. 4).

Considering an equilibrium on the starting material first, a perturbation of the initial absorbance A_0 could result from equilibration of the minor component **JOH** with CHP as in

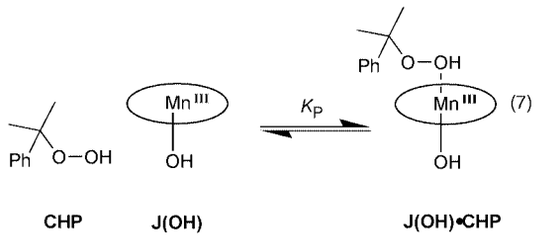

equilibrium (7). The exact binding mode of the CHP is not specified as the structure of the short-lived intermediate **JOH**·CHP (with absorbance A_0) cannot be interrogated.

Addition of CHP to impure Jacobsen's catalyst containing **JOH**, and in the presence of NMI, produces little change in absorbance just after addition of the CHP. It appears that there are insufficient differences in the absorption coefficients of the species in equilibrium (7) to account for the behaviour in the overall reaction. However, equilibrium (7) must be present to account for the dependence of the observed second-order rate constant k_2^{obs} with changing CHP concentration as no product **[J$_2$(O)]$^+$** is initially present in the reaction mixture. Combination of two **JOH**·CHP, generated *via* equilibrium (7), under second-order equal-concentration kinetics affords green **[J$_2$(O)]$^+$**. Defining this reaction in terms of the concentration of the impure Jacobsen's catalyst used [**JCl**$_{tot}$] (eqn. (5)) it can be shown (Supplementary data) that eqn. (8) applies. If K_P[CHP] $\ll$ 1,

$$k_2^{obs} = k_2^{true} \frac{[\text{“}\mathbf{JOH}\text{”}]}{[\mathbf{JCl}_{tot}]} \frac{K_P[\text{CHP}]}{(1 + K_P[\text{CHP}])} \qquad (8)$$

k_2^{obs} will increase linearly with the CHP concentration. With the concentrations of reagents used a linear plot of k_2^{obs} against [CHP] is obtained (Fig. 4) only if $K_P \approx 100$ M^{-1}.

An alternative explanation for the dependence of the absorbance rise on [CHP] is the presence of an equilibrium on the product **[J$_2$(O)]$^+$** through interaction with excess of CHP which is always present to give a more highly coloured product **[J$_2$(O)]$^+$**·CHP) as in equilibrium (9). The structure of such a

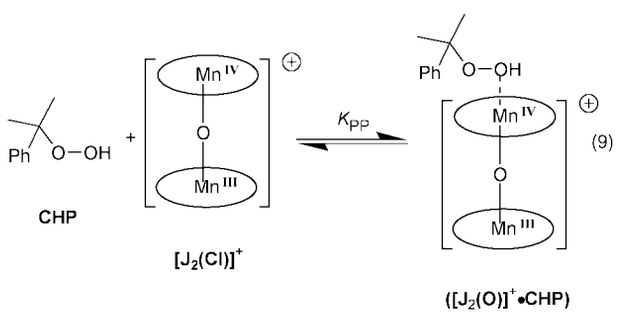

species is not known explicitly as the compound cannot be isolated. If equilibrium (9) can occur the change in absorbance is given by eqn. (10), where $a = \varepsilon_{P\cdot CHP}/\varepsilon_P$, **P** is the species **[J$_2$(O)]$^+$**

$$\Delta A = \frac{[\text{“}\mathbf{JOH}\text{”}]_0}{2}\left[\varepsilon_P\left(\frac{1 + aK_{PP}[\text{CHP}]}{1 + K_{PP}[\text{CHP}]}\right) - 2\varepsilon_{\text{“}\mathbf{JOH}\text{”}}\right] \qquad (10)$$

and **P**·CHP is **[J$_2$(O)]$^+$**·CHP. Fig. 3 shows that this equation fits the data well. The best-fit values of variables are K_{PP} 4000 M^{-1}, a 50, and ε_P 850 M^{-1} cm^{-1}, with [**JOH**] 3 × 10^{-5} M (initial [**JCl**$_{tot}$] 1 × 10^{-3} M). As required ε(**JOH**) is experimentally the same as ε(**JCl**) (270 M^{-1} cm^{-1} at 550 nm). Although further study is required to determine the constants more precisely, as eqn. (10) contains 5 variables, we have shown that the proposed interaction of CHP with **[J$_2$(O)]$^+$** can account for the experimental data.

Decay of intermediate [J$_2$(O)]$^+$. The green intermediate **[J$_2$(O)]$^+$** undergoes first-order decay in solution back to **JOH**.

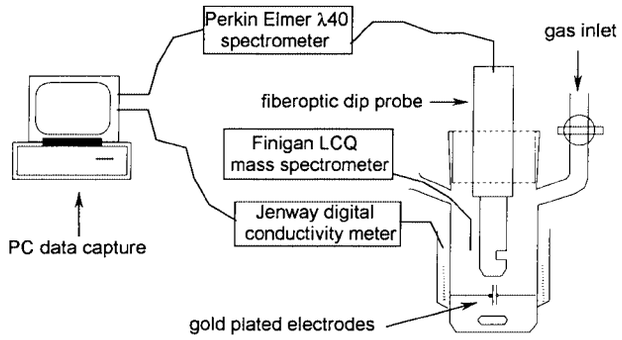

Fig. 5 Schematic view of the combined visible spectroscopy–conductance–electrospray MS cell.

No chemical decomposition of the salen complexes involved in the system occurs in these transformations and the formation of **[J$_2$(O)]$^+$** and its decay may be repeated at least six times on the same sample. However, it is apparent that Jacobsen's complex **JCl** itself undergoes photochemical decomposition with high intensity 550 nm light to afford non-absorbing species. Experiments conducted in a conventional Unicam UV3 UV/vis. spectrometer, where the sample was continuously irradiated with monochromatic 550 nm light, led to very slow first-order photochemical decay of 1 mM **JCl** solutions with $k_{photo} \approx 0.00003$ s^{-1}. Presumably this decomposition process follows the mechanism recently elucidated by Fukuda *et al.*[16] for analogous compounds. This photochemical decomposition could be avoided by working with the dip cell (Fig. 5) due to the much lower light intensity. Under these conditions the observed first-order rate constant for the decay of **[J$_2$(O)]$^+$** k_1^{obs} is 0.000250–0.000300 s^{-1}. It is very difficult to isolate the organic co-product(s) which are generated during the decomposition of intermediate **[J$_2$(O)]$^+$**, because of the very low concentrations used and the polar nature of the products generated. For reactions run under more concentrated conditions cumyl alcohol $PhCMe_2OH$ was the only product that could be identified. This product is normally indicative of Haber–Weiss hydroperoxide ROOH disproportionation,[20] a reaction for which Jacobsen's catalyst is known to be active in with H_2O_2.[21] As no oxygen evolution could be detected in any reaction the intermediate **[J$_2$(O)]$^+$** was intercepted with cyclohexene. GC analysis of the reaction mixture revealed that cyclohexenol and cyclohexenone were generated. The formation of such products is normally indicative of the formation of ROO$^\bullet$ and RO$^\bullet$ radicals derived from Haber–Weiss hydroperoxide decomposition.[20] Use of CHP-d_1, $PhCMe_2OOD$, in place of CHP did not significantly alter the rate of formation of **[J$_2$(O)]$^+$** or its decomposition. The decomposition of intermediate **[J$_2$(O)]$^+$** in the presence of an excess of Bu_4NCl was essentially unaffected indicating no chloride involvement.

Conclusions

The data from the combined visible spectroscopy, conductance, electrospray mass spectrometry suggest that Jacobsen's catalyst **JCl** reacts with σ-donor ligands to give labile Jahn–Teller distorted octahedral salts **[J(L)$_2$]Cl** as the major solution species. These labile compounds apparently react easily with OH$^-$ sources to give a hydroxy impurity **JOH**. This species **JOH** appears to be a minor contaminant in many samples of **JCl**. Given the ease with which **JCl** scavenges hydroxide sources typical **JCl**/NaOCl alkene epoxidation reactions[2] run at pH ≈ 11 will involve significant contribution by **JOH** to the catalytic manifold. Both in the presence and absence of NMI, **JOH** reacts with cumyl hydroperoxide to give a new product **[J$_2$(O)]$^+$**, suggested to be the mixed valence oxo bridged manganese(III,IV) dimer **[(μ-O)J$_2$]$^+$**. The behaviour of **[J$_2$(O)]$^+$** is complicated by the presence of equilibria with CHP involving

either the starting material **JOH** and/or the product itself. The species $[(\mu\text{-O})J_2]^+$ undergoes one electron reduction with an excess of CHP regenerating **JOH**. The cumyl radicals ROO$^\bullet$ and RO$^\bullet$ (R = $PhCMe_2$) generated in this chemistry undergo typical C–H abstraction reactions with cyclohexene. Overall, the reaction is best described as a cumyl hydroperoxide CHP disproportionation as shown in Scheme 3. The inability of the $[(\mu\text{-O})J_2]^+$

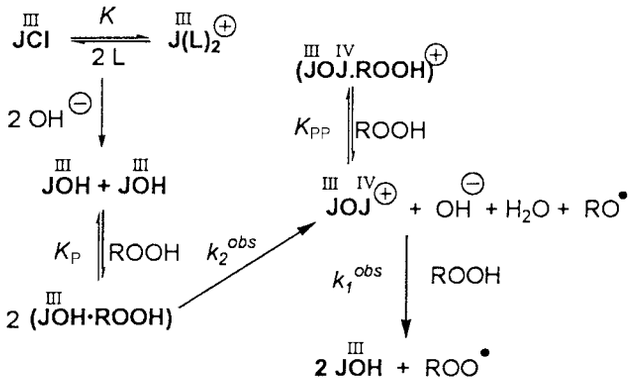

Scheme 3

to form a manganese(IV) dimer on treatment with CHP is the reason for the lack of epoxidation activity in attempted catalysis by **JCl**.

Experimental

General

All manipulations involving air or moisture sensitive reagents were carried out under nitrogen or argon atmospheres using standard Schlenk techniques. *N*-Methylimidazole (99%+, Aldrich) was distilled from CaH_2 under reduced pressure and stored under nitrogen at room temperature over A4 molecular sieves. Acetonitrile solutions of $HNMI^+Cl^-$ were prepared by addition of standard solutions of HCl gas in acetonitrile. Acetonitrile (HPLC grade) was distilled from CaH_2 immediately prior to use. Cyclohexene was distilled from anhydrous potassium carbonate. Tetrabutylammonium chloride (Fluka, >99%) was used as supplied and handled in a glovebag to prepare standard acetonitrile solutions of Bu_4NCl. A commercial source of 1.0 M Bu_4NOH in methanol (Aldrich) was used as supplied. Mass spectra were obtained either on a Finnigan 1020 (electron impact ionisation, EI) or a LCQ instrument (electrospray ionisation, ES; a capillary temperature of 200 °C was used together with the standard positive ionisation settings supplied with the instrument software). Proton NMR spectra were recorded on a JEOL-270 (270 MHz) spectrometer, visible spectra with Unicam UV3 (pathlength 1 cm) and Perkin-Elmer Lambda 40 (equipped with a Helma dipcell, pathlength 0.5 cm) instruments. Reaction compositions were analysed by GC using a Perkin-Elmer 8320 chromatograph equipped with a 24 m capillary BP-20 column, with the following parameters: oven temperature = 100 °C, injection temperature = 100 °C, detector temperature = 250 °C. Samples of Jacobsen's manganese salen complex **JCl** were either commercial (Aldrich) or prepared by a literature route.[18] Pure **JCl** gave no significant absorption change at 550 nm on treatment with NMI/CHP mixtures and was deemed to be free of hydroxide impurities (**JOH** and/or OH^-).

Purification of cumyl hydroperoxide

The method of Rosenthal *et al.*[22] was employed. Typically 4 grams of crude cumene hydroperoxide (technical grade, 80%) were dissolved in an equal volume of benzene and the organic layer washed with water (10 cm^3) three times. The organic layer was separated and distilled (0.1 mmHg) giving low boiling fractions (bp 20–40 °C) consisting of water and water/benzene/cumene hydroperoxide azeotropes. The pure hydroperoxide distilled as a sharp cut (bp 60–65 °C) which assayed as pure by ^1H NMR spectroscopy and iodometric titration.[23] The compound $PhCMe_2OOD$, CHP-d_1 was prepared by stirring similar CHP/benzene/D_2O mixtures in the presence of NaOH (35 mg) and employing a similar work-up. **CAUTION**: although no problems were encountered using these approaches, only small amounts of CHP (<5 g) should be purified at any one time. The method of Perrin[24] should not be used as explosions have been reported.[25]

Apparatus: general comments

Combined visible spectroscopy–conductance–electrospray mass spectrometry studies have not been described before; appropriate apparatus is shown schematically in Fig. 5. For meaningful conductance data to be attained rigorously anhydrous organic solvents were required. Additionally only systems containing sufficient charge carriers gave reliable conductance data. If these requirements were not adhered to then the measured conductance was dominated by residual water contamination. Both these requirements were met by solutions of **JCl** in freshly distilled acetonitrile. The usual platinum black electrodes used for conductance are not appropriate for oxidation reactions involving hydroperoxide intermediates, due to rapid ROOH disproportionation. However, gold-plated platinum electrodes could be used as the surface is completely passivated towards ROOH (R = H or alkyl) decomposition. Such cells cannot apparently be calibrated using standard aqueous KCl solutions (for which accurate values of the specific conductance κ are known[26]) due to electrochemical reactions at the gold surface. To check the behaviour of the combined technique cell, and allow absolute calibration in the case of conductance, some experiments were also run in parallel using traditional bench-top spectrometers and conductance cells.

Construction of the reaction cell. The glass reaction cell (volume *ca.* 20 cm^3) was fabricated to the general design of Fig. 5. The two approximately 1 cm^2 platinum electrodes were made from 0.207 mm thick plate (8/1000 in) cut to 14 × 7 mm. These were attached to platinum mounting wires, 0.503 mm in diameter (20/1000 in) with high temperature solder. The electrodes were mounted in the cell separated at a fixed distance (*ca.* 0.2 cm). The platinum plates and their supporting wires were completely passivated by being coated with gold using the aqueous electrolyte $K[Au(CN)_2]$ and passing a current of about 10 milliamps (see later). The plating efficiency was tested by using H_2O_2 which is much more sensitive to platinum-catalysed decomposition than cumene hydroperoxide used in these studies; no decomposition to H_2/O_2 could be detected (gas evolution or iodometric titration[21] of remaining H_2O_2). The platinum electrodes were connected *via* mercury pools to a Jenway 4320 digital conductance meter calibrated against 100 and 1000 Ω 0.1% wire-wound resistors. The cell constant was 0.82 cm^{-1}. The reaction cell has provision for controlled addition of gas if this becomes a requirement of the experiment. Similarly, samples may be withdrawn to an electrospray mass spectrometer by a Dosca micrometering pump. The cell mixture can be stirred with a mini-magnet flea and is theromostatted (±1 °C). The cell is fitted with a Helma fibre-optic dip probe (path length 5 mm) for concurrent measurement of absorbance.

Gold electroplating. The conductance cell having the platinum plates to be gold plated was cleaned with 33% neat HNO_3 that had been diluted with an equal volume of distilled water. The cell containing 15% w/w HNO_3(aq) was placed in an ultrasonic bath (10–15 min) then washed several times with distilled water. The gold plating solution was composed of 0.227 mM $K[Au(CN)_2]$ (20 cm^3) in the presence of monosodium citrate (0.01 M, 5 cm^3) and citric acid (0.01 M, 5 cm^3). The cell was kept in a water bath at 60–65 °C and the solution was

stirred. An electric current of 10 milliamps was passed for 20 minutes using a 4.5 V battery, a variable resistor, and milliamp meter.

Determination of equilibrium binding constants between Jacobsen's catalyst JCl and *N*-methylimidazoles (NMI, 1,2-DMNMI, 5Cl-NMI) or pyridines (Py, DMAP) or 4-phenylpyridine *N*-oxide (4-PhPyO)

By visible spectroscopy. Studies were carried out using either a thermostatted (25 ± 0.5 °C) Unicam UV3 or in the custom cell (Fig. 5) using a Perkin-Elmer Lambda 40 spectrometer. For the Unicam, five standard aliquots of *N*-methylimidazole NMI (6 μL, 75 μmol) were added to a 1.0 mM acetonitrile solution of Jacobsen's catalyst, **JCl** (3 cm^3, 0.003 mmol) in a glass cuvette in air. For the Perkin-Elmer five samples of *N*-methylimidazole NMI (20 μL, 75 mmol) were added to a 20 cm^3 of 1.0 mM of Jacobsen's catalyst **JCl** in acetonitrile. The equilibrium constant was calculated by the change in absorption at 500 or 550 nm. Other substituted imidazoles, pyridines, and 4-phenylpyridine *N*-oxide were investigated in a similar manner.

By conductivity. Studies were carried out as single experiments using a standard cell equipped with platinum black electrodes, or simultaneously with visible spectroscopy investigations using the custom cell (Fig. 5). In both cases a digital conductance meter calibrated against 100 and 1000 Ω 0.1% precision wire-wound resistors was used.

The standard conductance cell (volume 15 cm^3) contained two approximately 1 cm square platinum black electrodes at a fixed distance (*ca*. 0.2 cm). The cell was thermostatted at 20 or 25 °C. The cell constant, *b*, was determined by calibration against 0.01 M aqueous KCl using standard values of κ for KCl.[7] Specific conductances were determined using $\kappa = bC$, where *C* is the measured conductance and *b* the cell constant. In a typical run five standard aliquots of *N*-methylimidazole (20 μL, 0.25 mmol) were added to a 1.0 mM acetonitrile solution of Jacobsen's catalyst **JCl** (10 cm^3, 0.01 mmol total). Control runs indicated the change in the specific conductance of dry acetonitrile alone due to the addition of an equivalent amount of *N*-methylimidazole were at least five times smaller than for an acetonitrile solution of Jacobsen's catalyst **JCl** or at least 50 times smaller for solutions of Jacobsen's catalyst **JCl** in the presence of *N*-methylimidazole.

Studies in the gold UV-vis conductance cell (Fig. 5) were carried out in an identical manner except that the cell constant *b* had to be determined using the standard values of κ derived for Jacobsen's catalyst measured above as aqueous KCl solutions were found not to be suitable for calibrating gold cells.

Reaction of Jacobsen's complex JCl samples containing JOH with cumyl hydroperoxide in the presence of *N*-methylimidazole

Some visible spectroscopy studies were carried out using a thermostatted (20 ± 0.5 °C) Unicam UV3 spectrometer in air. Neat *N*-methylimidazole (30 μL, 0.0375 mmol) was added to a 1.0 mM MeCN solution of Jacobsen's catalyst **JCl** (3 cm^3, 0.0003 mmol total) in a glass cuvette and the solution shaken. The sample was placed in the spectrometer beam, the light turned to 550 nm and the absorbance zeroed. The data acquisition was started (absorbance, time data points every 10 s). After *ca*. 5 minutes a standard solution of cumyl hydroperoxide (30 μL 0.1 M in acetonitrile, 0.003 mmol) was added and the solution mixed rapidly with a plastic plunger. Typically data were recorded for 4–6 h. An infinity reading was taken at approximately 16 h. Similar runs were carried out varying the concentrations of the catalyst **JCl**, the *N*-methylimidazole and the cumyl hydroperoxide.

Additional runs were performed by monitoring visible spectroscopy and conductance simultaneously in the custom cell using the Perkin-Elmer instrument. Neat *N*-methylimidazole (200 μL, 2.51 mmol) was added to a 1.0 mM MeCN solution of Jacobsen's catalyst (20 cm^3, 0.02 mmol). The absorbance at 550 nm was monitored as a function of time. The residual absorbance of the MeCN solvent was removed by subtraction. Data acquisition was started and time–absorbance data points taken every 1 to 30 seconds. If necessary Bu_4NOH (0.001 to 0.008 mmol, as 1 M solution in MeOH) was added. After 5 minutes a standard solution of cumyl hydroperoxide (200 μL of 0.1 M MeCN solution, 0.02 mmol) was added. The mixture was thermostatted at 20 ± 0.5 °C with continuous stirring. Typically data both for spectral changes and conductance changes were recorded simultaneously every 30 seconds for 5 hours, or every second for 20 minutes. Similar runs were carried out varying the concentration of cumyl hydroperoxide, *N*-methylimidazole and catalyst **JCl**.

Interception of intermediate $[J_2(O)]^+$ with cyclohexene, *N*-methylimidazole hydrochloride or tetrabutylammonium chloride

The green intermediate $[J_2(O)]^+$ was generated in the usual way from 1 mM Jacobsen's catalyst **JCl**, 125 mM *N*-methylimidazole and 1 mM cumyl hydroperoxide. As the intermediate reached its maximum concentration (*ca*. 6 minutes after addition of cumyl hydroperoxide) standard solutions of neat cyclohexene, *N*-methylimidazole hydrochloride, or tetrabutylammonium chloride were added and mixed with plastic plunger (if using the Unicam UV3) or by stirrer bar (if using the Perkin-Elmer instrument). Absorbance/time data were collected in the normal way. In the case of cyclohexene, 2-cyclohexanone was detected as the sole oxidation product by GC (BP-20 column, 100 °C isothermal).

Acknowledgements

We thank the EPSRC (GR/L48430) and Royal Society for financial support for equipment and the Pakistan government for a studentship (to S. A. K.). We are grateful to Drs Frank Mabbs and David Coulison for recording EPR spectra of reaction mixtures. Mike Bailey, Terry Aspinwell, Eric Davies, and Jed McPartland made valuable contributions to instrument construction.

References

1 Reviews: L. Canali and D. C. Sherrington, *Chem. Soc. Rev.*, 1999, **28**, 85; T. Katsuki, *Coord. Chem. Rev.*, 1995, **140**, 189.
2 Notable examples: L. Deng and E. N. Jacobsen, *J. Org. Chem.*, 1992, **57**, 4320; M. Palucki, N. S. Finney, P. J. Pospisil, M. L. Guler, T. Ishida and E. N. Jacobsen, *J. Am. Chem. Soc.*, 1998, **120**, 948.
3 P. Pietikäinen, *Tetrahedron Lett.*, 1994, **35**, 941; M. Palucki, P. Hanson and E. N. Jacobsen, *Tetrahedron Lett.*, 1992, **33**, 7111.
4 P. Pietikäinen, *Tetrahedron Lett.*, 1995, **36**, 319.
5 M. Palucki, G. J. McCormick and E. N. Jacobsen, *Tetrahedron Lett.*, 1995, **36**, 5457.
6 K. Srinvasan, P. Michaud and J. K. Kochi, *J. Am. Chem. Soc.*, 1986, **108**, 2309; K. Srinivasen, S. Perrier and J. K. Kochi, *J. Mol. Catal.*, 1986, **36**, 297.
7 D. Feichtinger and D. A. Plattner, *Angew. Chem.*, *Int. Ed. Engl.*, 1997, **36**, 1718.
8 D. Bell, M. R. Davies, F. J. L. Finney, G. R. Geen, P. M. Kincey and I. S. Mann, *Tetrahedron Lett.*, 1996, **37**, 3895; D. L. Hughes, G. B. Smith, J. Liu, G. C. Dezeny, C. H. Senanayake, R. D. Larsen, T. R. Verhoeven and P. J. Reider, *J. Org. Chem.*, 1997, **62**, 2222; J. Skarzewski, A. Gupta and A. Vogt, *J. Mol. Catal. A*, 1995, **130**, L63.
9 F. E. Mabbs and D. Collison, in *Electron Paramagnetic Resonance of d Transition Metal Compounds*, Studies in Inorganic Chemistry, Elsevier, London, 1992.
10 F. Jiang, J. McCracken and J. Peisach, *J. Am. Chem. Soc.*, 1990, **112**, 9035.
11 R. M. Smith and A. E. Martell, in *Critical Stability Constants*, Plenum, New York, 1975, vol. 2.
12 A. E. Martell and R. M. Smith, in *Critical Stability Constants*, Plenum, New York, 1982, vol. 5.

13 A. R. Katrizky and P. Simmons, *J. Chem. Soc.*, 1960, 1511.
14 M. R. Bermejo, M. Fondo, A. Garcia-Deibe, M. Rey, J. Sanmartin, A. Sousa, M. Watkinson, C. A. McAuliffe and R. G. Pritchard, *Polyhedron*, 1996, **15**, 4185.
15 P. J. Pospisil, D. H. Carsten and E. N. Jacobsen, *Chem. Eur. J.*, 1996, **2**, 974; W. Zhang, J. L. Loebach, S. R. Wilson and E. N. Jacobsen, *J. Am. Chem. Soc.*, 1990, **112**, 2801.
16 T. Fukuda, F. Sakamoto, M. Sato, Y. Nakano and Y. Fujii, *Chem. Commun.*, 1998, 1391.
17 A. Bettelheim, D. Ozer and D. Weinraub, *J. Chem. Soc.*, *Dalton Trans*, 1986, 2297; M. J. Camenzind, B. C. Schardt and C. L. Hill, *Inorg. Chem.*, 1984, **23**, 1984; B. C. Schardt, F. J. Hollander and C. L. Hill, *J. Am. Chem. Soc.*, 1982, **104**, 3964.
18 L. Deng and E. N. Jacobsen, *J. Org. Chem.*, 1992, **57**, 4320.
19 K. Oyaizu, A. Haryono, H. Yonemaru and E. Tsuchia, *J. Chem. Soc.*, *Faraday Trans.*, 1998, 3393.
20 R. A. Sheldon and J. K. Kochi, in *Metal-Catalysed Oxidations of Organic Compounds*, Academic Press, New York, 1981.
21 E. N. Jacobsen, W. Zhang and L. Deng, *PTC Int. Appl. WO*, 93038338, 4 March 1993 (*Chem. Abstr.*, 1994, **120**, 7876v).
22 R. Rosenthal, M. N. Sheng and J. G. Zajacek, Atlantic Richfield Co., *US Pat.* 3639486, 15 December 1967 (*Chem. Abstr.*, 1972, **76**, 85550w).
23 S. Woodward, in *Transition Metals in Organic Synthesis—A Practical Approach*, ed. S. E. Gibson (née Thomas), Oxford University Press, Oxford, 1997.
24 D. D. Perrin, W. L. F. Armarego and D. R. Perrin, in *Purification of Laboratory Chemicals*, 2nd edn., Pergamon Press Ltd., Oxford, 1980, p. 181.
25 M. A. Francisco, *Chem. Eng. News*, 1993, **71**(22), 4; H. E. Hood, *Chem. Eng. News*, 1993, **71**(42), 4.
26 W. G. Palmer, in *Experimental Physical Chemistry*, Cambridge University Press, Cambridge, 1954, ch. 6, pp. 182–188.

Paper b001059f